Chinese Chemical Letters 34 (2023) 107786

Contents lists available at ScienceDirect

Chinese Chemical Letters

journal homepage: www.elsevier.com/locate/cclet

GSH responsive traditional clinical drugs probe for cancer cell fluorescence imaging and therapy

Jie Xing[a,b,c,1], Qiuyu Gong[a,1], Ruifen Zou[a,b], Junlie Yao[a,b,c], Lingchao Xiang[a,b], Aiguo Wu[a,b,*]

[a] Cixi Institute of Biomedical Engineering, International Cooperation Base of Biomedical Materials Technology and Application, Chinese Academy of Science (CAS) Key Laboratory of Magnetic Materials and Devices and Zhejiang Engineering Research Center for Biomedical Materials, Ningbo Institute of Materials Technology and Engineering, CAS, Ningbo 315201, China

[b] Advanced Energy Science and Technology Guangdong Laboratory, Huizhou 516000, China

[c] University of Chinese Academy of Sciences, Beijing 100049, China

ARTICLE INFO

Article history:
Received 20 December 2021
Revised 17 August 2022
Accepted 24 August 2022
Available online 28 August 2022

Keywords:
Methylene blue
GSH response
Fluorescent probe
Fluorescence imaging
Photodynamic therapy

ABSTRACT

Despite the rapid development of fluorescence detection modalities for disease diagnosis, novel fluorescent molecules and probes still face with tremendous pressure to transform before employing such fluorescent tools in the clinic. Impressively, the fluorescent probes based on the traditional fluorescent dye are expected to accelerate the transformation process. Herein, methylene blue is requisitioned to design the GSH responsive probe **MB-SS-CPT** elaborately. The as-synthesized **MB-SS-CPT** provides a dramatic optical advantage for GSH detection *in vitro*, cell fluorescence imaging, *in vivo* imaging, and antitumor therapy.

With the increasing aging of the population, the incidence rate of cancer has increased year by year, and it has greatly threatened human health [1]. Therefore, effective diagnosis and treatment of cancer is a major task facing the world scientists. In recent years, cancer-related fluorescent diagnostic probes have sprung up in the fields of surgical navigation, *in vitro* diagnosis and prognostic analysis [2–4]. It is well known that fluorescence diagnosis has fast, noninvasive and high temporal and spatial resolution [5,6]. Compared with inorganic fluorescent diagnostic probe, organic fluorescent diagnostic probe has numerous characteristics including small molecular weight, degradability and the performance to be quickly removed by organism metabolism [7–9]. In light of these, a large number of novel organic fluorescent dye groups have been invented, such as high quantum yield, near-infrared emission wavelength, and ultra-high photothermal conversion efficiency, which provide the basis for new fluorescent diagnosis and treatment probes [10–14]. Nevertheless, the clinical transformation of fluorescent probes is still slow, and the types of fluorescent dyes approved by FDA still change little. Therefore, many scientists design fluorescent diagnostic probes for cancer diagnosis and treatment based on the traditional clinical use of fluorescent dyes [15–17].

Methylene blue (MB) has previously been widely used in clinic, such as injecting methylene blue during surgery to help find lymphnodes, diagnosis and photodynamic therapy of breast cancer and head and neck cancer [18–22]. Recently, some researchers also found that MB has a new function of enhancing immunotherapy in antitumor therapy [23]. Its longer wavelength excitation and emission fluorescence (λ_{ex}: 660 nm, λ_{em}: 690 nm) and photodynamic properties have attracted attention [24]. We envisage to further improve its application scope through reasonable design, developments of responsive fluorescent probes, and realizing the integration of diagnosis and treatment.

Endogenous thioalcohol glutathione (GSH) is usually overexpressed in cancer cells. Many special groups that can react with GSH have been reported [14,25–31]. Among these responsive groups, disulfide bond is a classical chemical bond in response to GSH, the design strategy of using disulfide bond is much higher than others. The main application field is the design of prodrug probe, which can reduce the side effects of chemotherapy drugs through the targeted release of drugs with high GSH specific response [32,33]. In the study of prodrug strategy, there are many prodrugs fluorescent probes taking Camptothecin (CPT) as an example [34–37]. Among those probes, the fluorophores usually play

* Corresponding author at: Cixi Institute of Biomedical Engineering, International Cooperation Base of Biomedical Materials Technology and Application, Chinese Academy of Science (CAS) Key Laboratory of Magnetic Materials and Devices and Zhejiang Engineering Research Center for Biomedical Materials, Ningbo Institute of Materials Technology and Engineering, CAS, Ningbo 315201, China.

E-mail address: aiguo@nimte.ac.cn (A. Wu).

[1] These authors contributed equally to this work.

https://doi.org/10.1016/j.cclet.2022.107786
1001-8417/

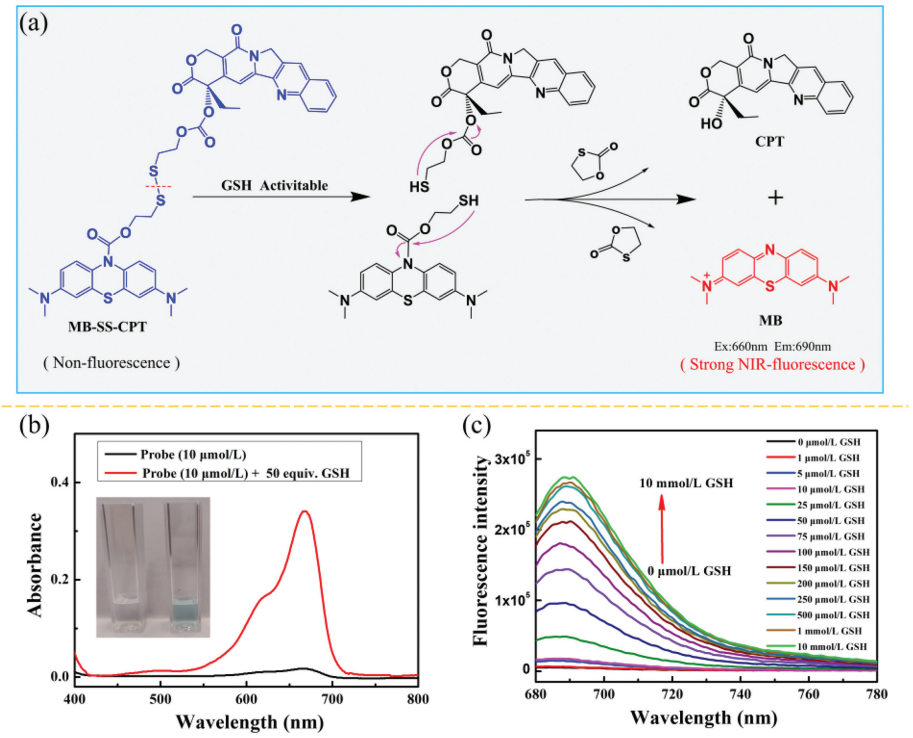

Fig. 1. (a) The mechanism scheme of MB-SS-CPT responds to GSH. (b) UV-vis absorption spectra of probe (10 μmol/L) before/after incubation with 500 μmol/L GSH. (c) Fluorescence spectra of 10 μmol/L probe upon the addition of GSH (0–10 mmol/L).

a fluorescent signal to monitor drug release, but lack significant therapeutic functions. Therefore, we selected disulfide bond and connected MB to prepare the probe **MB-SS-CPT**, which integrates the functions of high GSH response, chemotherapy and photodynamic therapy. In addition, it is characterized of low-cost raw material and wide clinical application of fluorophore (MB) and chemotherapeutic drug (CPT).

It is found that the modification at the 10-N position of MB can change from blue to colorless, and carbamoyl linkage can make MB have switching performance [16]. At this special site, the probe **MB-SS-CPT** is obtained by connecting chemotherapeutic drugs with triphosgene through disulfide bond. The fluorescent diagnosis and treatment function of **MB-SS-CPT** are realized by releasing CPT and MB through GSH breaking the disulfide bond inside the molecule shown in Fig. 1a. The synthesis of **MB-SS-CPT** required two steps, and the detailed synthesis route was shown in Scheme S1 (Supporting information). After **MB-SS-CPT** was synthesized, its structure was confirmed by ^{1}H NMR, ^{13}C NMR, high-resolution mass spectrometry (Figs. S1–S3 in Supporting information). In Fig. 1b, the probe solution of 10 μmol/L is colorless and transparent, and there is no characteristic peak in UV absorption. After incubation with 50 equiv. GSH solution for 4 h at this concentration, the solution can be observed to turn blue. And as well UV absorption spectrum shows the same characteristic peak as MB at 666 nm.

In order to confirm the occurrence of chemical reaction, MB, CPT and their derivatives in the mixture after reaction were detected by high-resolution mass spectrometry (Fig. S5 in Supporting information). These experimental results show that the disulfide bond of **MB-SS-CPT** could be cleaved by GSH, thus realizing the release of colored MB. In order to obtain the optimum incubation time with GSH *in vitro*, 25 and 50 equiv. GSH concentrations were selected to test the response time curve (Fig. S6 in Supporting information). The co-incubation time to reach the fluorescence intensity plateau is about 60 min when the GSH concentration is 50 equiv., while it takes a longer time (about 120 min) once the GSH concentration reduces to 25 equiv. (optimum incubation temperature at 37 °C in Fig. S7 in Supporting information). Therefore, in the fluorescence spectrum test for detecting different concentrations of GSH, the incubation time was set to 4 h to ensure that the reaction time of all concentrations with 10 μmol/L probe is sufficient. The fluorescence spectrum of the solution after reacting with 0–10 mmol/L of GSH shown in Fig. 1c. Overall, the fluorescence intensity increases with the increase of GSH concentration (0–10 mmol/L), and there is a linear relationship in the range of 0–10 equiv. concentration of GSH (Fig. S4 in Supporting information), based on the formula LOD = 3 δ/K, the lowest detection concentration of **MB-SS-CPT** for GSH is calculated as 820 nmol/L.

Before MB-SS-CPT was applied to cells, we first tested the selectivity of **MB-SS-CPT** and incubated the probe with candidate interfering substances such as amino acids and metal ions in solution. In Fig. S8 (Supporting information), the fluorescence shows that the fluorescence intensity of cysteine (Cys) and GSH is almost the same after the reaction. This is a reasonable result because they have similar structure and function of breaking disulfide bonds. FBS (Fetal Bovine Serum) is composed of many substances like proteases, so **MB-SS-CPT** has less response, which is also expected. The other amino acids, glucose, ascorbic acid, Mg^{2+}, Ca^{2+} and other substances did not increase the fluorescence intensity and UV absorption of **MB-SS-CPT**, and the color of the solution was still colorless. This shows that **MB-SS-CPT** has strong selectivity for GSH and Cys. The concentration of GSH in tumor cells and their microenvironment is much higher than that of Cys, so will not be disturbed in the application of *in vivo* imaging.

The function of cancer cell fluorescence imaging is one of the important applications of **MB-SS-CPT**. Breast cancer cell line 4T1 and esophageal cancer cell line KYSE 30 were used as model cells to test the fluorescence imaging ability of **MB-SS-CPT**. Fig. 2a is the confocal fluorescence imaging picture of 4T1 cells which intuitively shows that 10 μmol/L probe incubated with cells for 2 h will

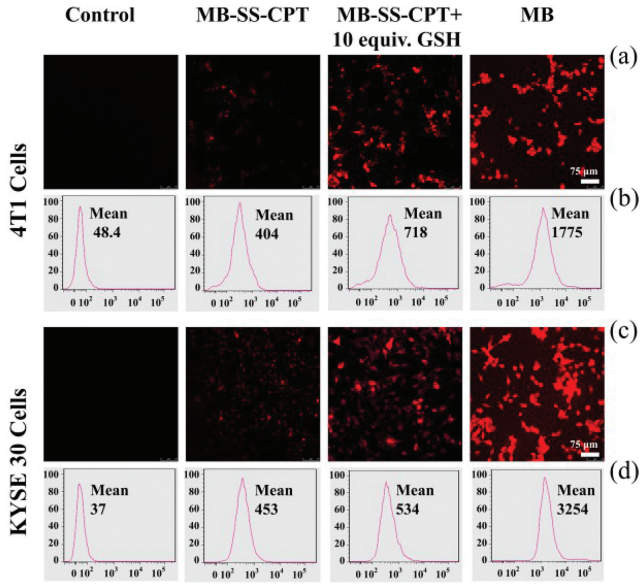

Fig. 2. The fluorescence response of **MB-SS-CPT** to GSH concentration at the cell level. (a, b) Fluorescence imaging and flow cytometry of probe **MB-SS-CPT** (10 μmol/L) in 4T1 cell line. (c, d) Fluorescence imaging and flow cytometry of probe **MB-SS-CPT** (10 μmol/L) in KYSE 30 cell line.

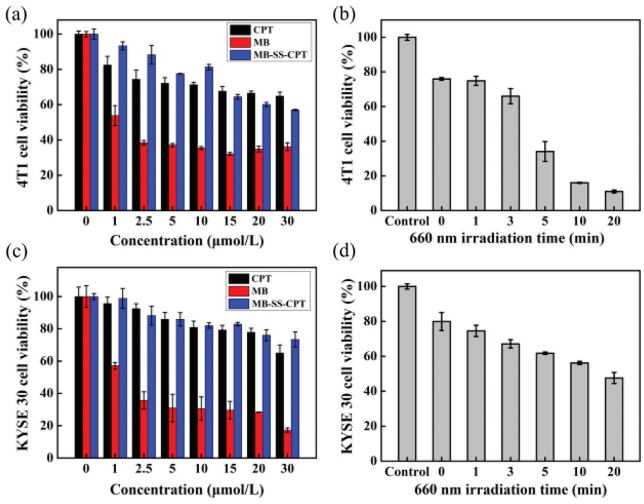

Fig. 3. (a, b) Dark toxicity of three substances and photodynamic therapy on 4T1 cells. (c, d) Dark toxicity of three substances and photodynamic therapy of **MB-SS-CPT** in KYSE 30 cells.

have a certain fluorescence intensity. After the addition of exogenous GSH, the cell fluorescence intensity significantly enhanced. There are two control groups at both ends: negative (**MB-SS-CPT** 0 μmol/L) and positive (MB 10 μmol/L). The statistical results of flow cytometry fluorescence intensity in Fig. 2b correspond to the fluorescence imaging picture. Figs. 2c and d also show that **MB-SS-CPT** can be used as a fluorescence detection tool in fluorescence imaging and flow cytometry of esophageal cancer cells.

Since **MB-SS-CPT** is a theranostic probe integrating fluorescence imaging and antitumor therapy, next, we looked at its therapy function. The two cell lines previously imaged were still selected. Figs. 3a and c tested the dark toxicity of three substances CPT, MB and **MB-SS-CPT**. After the tested materials were incubated with cells for 24 h, **MB-SS-CPT** displayed better cell viability than MB and CPT, which indicated that **MB-SS-CPT** was less toxic and safer under no light conditions. The survival rate of cells showed that the toxicity of free MB increased with the increase of concentration. As a chemotherapeutic drug, CPT does not show strong killing effect in here, which is reasonable, because our incubation time is less than 48 h [38,39]. Fig. 3b shows the cell survival after **MB-SS-CPT** to 4T1 cells for 4 h and irradiated with 660 nm laser with constant concentration and power (10 μmol/L, 100 mW) for different times. The mortality of 4T1 cells after irradiation for more than 10 min exceeded 80%. Under the same conditions, the mortality of esophageal cancer cell KYSE 30 was only 40% in Fig. 3d. In view of the more significant killing effect of **MB-SS-CPT** on 4T1 cells, the tumor model established by 4T1 cells was selected for subsequent *in vivo* tumor model imaging and therapeutic application research.

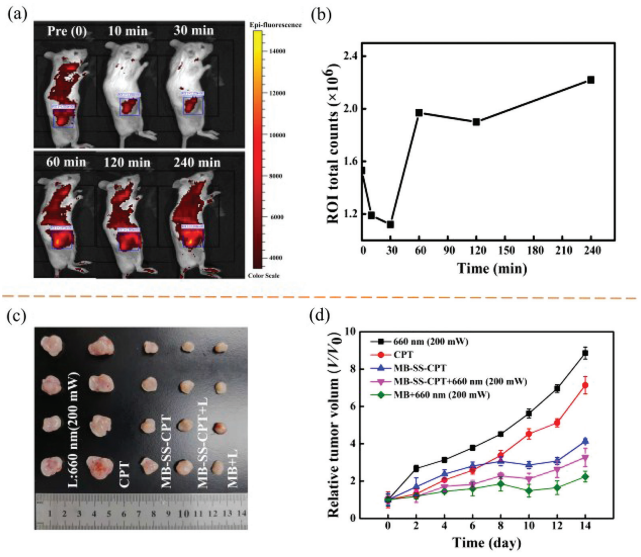

Fig. 4. (a, b) **MB-SS-CPT** *in vivo* imaging and intensity curve of mouse breast cancer 4T1 xenograft model. (c) Tumors separated from the experiment mice. (d) Tumor volume change curve.

We evaluated the *in vivo* safety of CPT, MB and **MB-SS-CPT** before *in vivo* imaging and treatment. In Fig. S9 (Supporting information), H&E staining results of important organs were not significantly different from those of control group injected PBS, indicating that our MB-SS-CPT is safe for mice under these doses.

The high level of GSH concentration at the tumor site can make the probe turn-on [40,41]. When MB-SS-CPT was injected into near the tumor, Figs. 4a and b show that the change of fluorescence intensity of tumor with time. The platform period begins to appear in 60 min after **MB-SS-CPT** was injected, the signal-to-noise ratio is doubled and maintained for more than 3 h. This imaging time result provides a reference for the next photodynamic therapy policy. After **MB-SS-CPT** was injected locally for 4 h, the tumor site was irradiated with 660 nm for photodynamic therapy. In Figs. 4c and d, after three times of irradiated treatment, the *in vitro* tumor size and monitoring volume curve show that the tumor inhibition rate of **MB-SS-CPT** reached 60% compared to control group, which was equivalent to the effect of free MB group. There was no significant change in the body weight of mice in the five groups during the treatment (Fig. S10c in Supporting information). Animal experiments show that **MB-SS-CPT** not only had the photodynamic treatment function close to MB, but also had the fluorescence imaging performance of GSH tumor site response.

In conclusion, we designed **MB-SS-CPT**, a fluorescent molecular probe based on traditional drugs, which has outstanding fluorescence response and selectivity in the detection of GSH solution *in vitro*, and the detection limit LOD = 820 nmol/L. **MB-SS-CPT** has a certain fluorescence imaging potential in breast cancer cells and esophageal cancer cell lines in response to GSH. As for *in vivo* imaging and photodynamic antitumor therapy, it also exhib-

ited satisfying performance comparing favourably with MB. Most importantly, both MB and CPT in **MB-SS-CPT** structure come from clinical drugs and have strong competitiveness in clinical transformation.

Declaration of competing interest

The authors declare that they have no known competing financial interests or personal relationships that could have appeared to influence the work reported in this paper.

Acknowledgments

This work was supported by the National Natural Science Foundation of China (Nos. 32025021, 31971292 and 51873225), National Key R&D Program of China (Nos. 2018YFC0910601 and 2019YFA0405603), the Key R&D project of Zhejiang Province (No. 2020C03110), and the Key Scientific and Technological Special Project of Ningbo City (Nos. 2017C110022 and 2020Z094). The authors gratefully acknowledge Miss Yingying Han for the high-resolution mass spectrum experiments. Furthermore, the authors also acknowledge National Synchrotron Radiation Laboratory in Hefei for High End User Cultivation Fund (No. 2020HSC-UE006) and Shanghai Synchrotron Radiation Facility at Line BL15U for X-ray fluorescence imaging.

Supplementary materials

Supplementary material associated with this article can be found, in the online version, at doi:10.1016/j.cclet.2022.107786.

References

[1] R.L. Siegel, K.D. Miller, H.E. Fuchs, A. Jemal, CA Cancer J. Clin. 71 (2021) 7–33.
[2] E. Upchurch, S. Griffiths, G.R. Lloyd, et al., Future Oncol. 13 (2017) 2363–2382.
[3] C.Z. Wu, J. Gleysteen, N.T. Teraphongphom, Y. Li, E. Rosenthal, Int. J. Oral Sci. 10 (2018) 10, doi:10.1038/s41368-018-0011-4.
[4] E. de Boer, N.J. Harlaar, A. Taruttis, et al., Br. J. Surg. 102 (2015) E56–E72.
[5] S. Favril, E. Abma, F. Blasi, et al., Vet. Rec. 183 (2018) 354.
[6] J. Xing, Q.Y. Gong, O.U. Akakuru, et al., Nanoscale 12 (2020) 24311–24330.
[7] X.H. Zhu, J. Zhang, J.L. Liu, Y. Zhang, Adv. Sci. 6 (2019) 1901358.
[8] W. Sun, M. Li, J.L. Fan, X.J. Peng, Acc. Chem. Res. 52 (2019) 2818–2831.
[9] C. Dong, S.N. Wang, M.H. Ma, et al., Appl. Mater. Today 25 (2021) 101178.
[10] H.X. Liu, L.H. Xiong, R.T.K. Kwok, et al., Adv. Opt. Mater. 8 (2020) 2000162.
[11] H. Zhou, Y.L. Xiao, X.C. Hong, Chin. Chem. Lett. 29 (2018) 1425–1428.
[12] N. Ding, Z. Li, X.W. Tian, et al., Chem. Commun. 55 (2019) 13172–13175.
[13] Y. Liu, Z.S. Li, L. Chen, Z.G. Xie, Dyes Pigment. 141 (2017) 5–12.
[14] C.X. Yan, L.M. Shi, Z.Q. Guo, W.H. Zhu, Chin. Chem. Lett. 30 (2019) 1849–1855.
[15] J. Cao, J.N. Chi, J.F. Xia, et al., ACS Appl. Mater. Interfaces 11 (2019) 25720–25729.
[16] H.M. Dao, C.H. Whang, V.K. Shankar, et al., Chem. Commun. 56 (2020) 1673–1676.
[17] H.G. Wei, Y.J. Liu, X.D. Zhao, Bioorg. Med. Chem. Lett. 30 (2020) 127221.
[18] J.Y. Li, X. Chen, M. Qi, Y.S. Li, PLoS One 13 (2018) e0204364.
[19] Y. Diab, Int. J. Gynecol. Cancer 27 (2017) 154–158.
[20] Y. Kumagai, K. Kawada, S. Yamazaki, et al., Dis. Esophagus 22 (2009) 505–512.
[21] C. Stefan, G. Lostun, A. Lostun, Rev. Chim. 68 (2017) 1222–1224.
[22] J.P. Tardivo, A. Del Giglio, C.S. de Oliveira, et al., Photodiagn. Photodyn. Ther. 2 (2005) 175–191.
[23] Z. Fan, Y. Tian, Z. Chen, et al., EMBO Mol. Med. 12 (2020) e11571.
[24] Y. Wen, F.J. Huo, J.P. Wang, C.X. Yin, J. Mater. Chem. B 7 (2019) 6855–6860.
[25] M.H. Lee, J.L. Sessler, J.S. Kim, Acc. Chem. Res. 48 (2015) 2935–2946.
[26] Y.K. Yue, F.J. Huo, C.X. Yin, Chem. Sci. 12 (2021) 1220–1226.
[27] Y.F. Huang, Y.B. Zhang, F.G. Huo, Y.M. Liu, C.X. Yin, Sens. Actuator. B: Chem. 301 (2019) 127123.
[28] W.J. Zhang, F.J. Huo, F.Q. Cheng, C.X. Yin, J. Am. Chem. Soc. 142 (2020) 6324–6331.
[29] Y.T. Yang, T.T. Zhou, M. Jin, et al., J. Am. Chem. Soc. 142 (2020) 1614–1620.
[30] X.J. Ren, L.D. Liao, Z.G. Yang, et al., Chin. Chem. Lett. 32 (2021) 1061–1065.
[31] Y.B. Zhang, Y. Zhang, Y.K. Yue, et al., Chin. Chem. Lett. 32 (2021) 2873–2876.
[32] X.Y. Song, X.Y. Han, F.B. Yu, et al., Theranostics 8 (2018) 2217–2228.
[33] J. Guan, Y. Wu, X. Liu, et al., Biomaterials 279 (2021) 121180.
[34] X.M. Wu, X.R. Sun, Z.Q. Guo, et al., J. Am. Chem. Soc. 136 (2014) 3579–3588.
[35] C.H. Whang, E. Yoo, S.K. Hur, et al., Chem. Commun. 54 (2018) 9031–9034.
[36] Z.Q. Guo, Y.G. Ma, Y.J. Liu, et al., Sci. China Chem. 61 (2018) 1293–1300.
[37] L. Qiu, L.F. Zhao, C.F. Xing, Y. Zhan, Chin. Chem. Lett. 29 (2018) 301–304.
[38] T. Zhang, X. Ma, S. Bai, et al., J. Mater. Chem. B 8 (2020) 1245–1255.
[39] Z.J. Chen, N. He, M.H. Chen, L. Zhao, X.H. Li, Acta Biomater. 43 (2016) 195–207.
[40] X.Y. Song, R. Wang, J.F. Gao, et al., Chin. Chem. Lett. 33 (2022) 1567–1571.
[41] L. Luo, Y. Qi, H. Zhong, et al., Acta Pharm. Sin. B 12 (2022) 424–436.